# Ferromagnetic Coupling Behavior in Oxo-Bridged Binuclear Bis($\eta^5$-cyclopentadienyl)titanium(III) Complex $(Cp_2Ti)_2(\mu$-O): A Density Functional Theory Combined with Broken-Symmetry Approach

**Qinghua Ren, Zhida Chen,* Jie Ren, Haiyan Wei, Wentao Feng, and Lei Zhang**

*Department of Chemistry, State Key Laboratory of Rare Earth Materials Chemistry and Applications, Peking University, Beijing 100871, China, and Peking University-The University of Hong Kong Joint Laboratory in Rare Earth Materials and Bioinorganic Chemistry, Beijing 100871, China*

*Received: November 29, 2001; In Final Form: May 1, 2002*

The ferromagnetic coupling behavior in oxo-bridged bis(bis(cyclopentadienyl)titanium(III)) complex $(Cp_2Ti)_2(\mu$-O) is investigated on the basis of calculations of density functional theory combined with the broken-symmetry approach. The magnetic coupling constants calculated for the experimental and optimized geometries are 11.41 and 1.29 $cm^{-1}$, respectively, comparable with the experimentally measured $J$ value (8.3 $cm^{-1}$). The calculated results show that the magnetic coupling constant $J$ slightly decreases with the increase of the Ti−($\mu$-O)−Ti angle and decreases exponentially with the increase of the Ti−($\mu$-O) distance. In variation of the dihedral angle $\beta$ between the two $Cp_2Ti$ fragments the transition of the magnetic coupling property occurs near $\beta = 45°$. For $\beta > 45°$, the coupling is ferromagnetic, and it is antiferromagnetic for $\beta < 45°$. The ferromagnetic coupling interaction between the magnetic centers is almost not affected by the protonation of the oxo-bridge ligand. Molecular orbital analysis reveals that, because of the nonbonding character and electronic location character of the single-occupied molecular orbitals (SOMO), there is no antiferromagnetic coupling pathway through superexchange via the bridging atom. However, when $\beta$ varies from 90° to 0°, the through-space interaction between the two magnetic centers in the SOMOs occurs, leading to a gradually increscent antiferromagnetic contribution, $J_{AF}$. As soon as the antiferromagnetic contribution exceeds the ferromagnetic contribution, $J_F$, the transition of the magnetic coupling properties for the molecule occurs. The spin population analysis is briefly discussed.

## Introduction

In molecular magnetism, the magnetostructural correlation of bridged transition metal dimers has received considerable attention, especially linear $\mu$-oxo-bridged homo-binuclear transition metal complexes, in which most magnetic exchange interactions between two magnetic centers exhibit antiferromagnetic character. Recently, the intriguing magnetic behavior of the form $L_5M-O-ML_5$ with early transition metals M = Ti, V, Cr in the oxidation state +3 aroused intensive interest,[1−3] in which the Ti complex is paramagnetic or only weakly antiferromagnetic with a small exchange integral and the V complexes are strongly ferromagnetic, whereas the Cr complexes are strongly antiferromagnetic. On the other hand, a number of binuclear bis($\eta^5$-cyclopentadienyl)titanium(III) complexes bridged by the diversified dianion B of saturated and unsaturated dicarboxylic acids have been reported.[4−6] These complexes have the composition $[[\eta^5\text{-}C_5H_5]_2Ti]_2B$. The variable-temperature magnetic susceptibility data show that these complexes have a weak intramolecular antiferromagnetic exchange interaction with the coupling constant, $J$, in the range 0−10 $cm^{-1}$. Honold et al.[7] have reported the molecular structure of the simplest binuclear titanium(III) metallocene, $(Cp_2Ti)_2(\mu$-O). Then, Lukens and Andersen[8] have studied the magnetic behavior for the molecule and found the intramolecular magnetic exchange to be ferromagnetic with a coupling constant $J$ of 8.3 $cm^{-1}$. To the best of our knowledge, this is the only bimetallic titanocene complex in which $d^1-d^1$ between the titanium centers are coupled ferromagnetically. Inspection of the idealized geometry for $(Cp_2Ti)_2(\mu$-O) shows[7] that the $(\eta^5\text{-}C_5H_5)_2Ti$ fragments in the molecule have a typically bent sandwich geometry with a staggered configuration of the two Cp rings and the dihedral angles between the planes of the Cp rings in a $(\eta^5\text{-}C_5H_5)_2Ti$ fragment are 136.0°, where distance of Cp−Ti is 2.067 Å. The Ti−O−Ti angle is 170.9° and the Ti−O distance is 1.838 Å. It is interesting to note that the cyclopentadienyl rings in a bent sandwich fragment are rotated 90° relative to another bent sandwich fragment (Figure 1). It is beyond any doubt that the salient magnetic behavior and structural feature for $(Cp_2Ti)_2(\mu$-O) are worth noting. What structural factor to determine the ferromagnetic coupling behavior in $(Cp_2Ti)_2(\mu$-O) aroused our great interest? In present paper, we pay more attention to the magnetostructural correlation and the magnetic exchange interaction pathway for the ferromagnetic coupling system $(Cp_2Ti)_2(\mu$-O).

## Computational Details

**Calculation on Exchange Coupling Constant.** As demonstrated in the previous reports,[9−16] the density functional method (DFT) is able to handle larger systems, and the broken-symmetry approach (BS) under the DFT framework, proposed by

* To whom correspondence should be addressed. Fax: +86-10-62751708. E-mail: zdchen@pku.edu.cn.

10.1021/jp014368+ CCC: $22.00 
Published on Web 05/24/2002

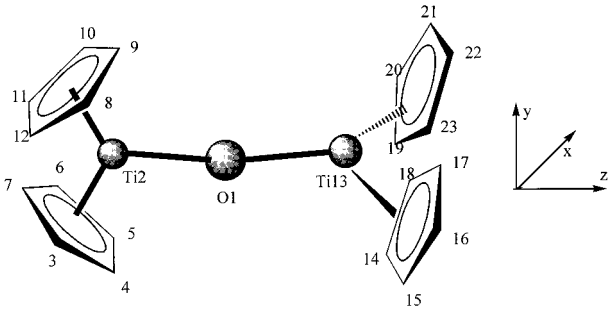


**Figure 1.** Molecular structure of $(Cp_2Ti)_2(\mu\text{-O})$.

Noodleman,[12−15] allows calculations of the exchange coupling constant of complex molecules with a good degree of accuracy. Therefore, in our calculations on the magnetic exchange interaction between titanium centers in $(Cp_2Ti)_2(\mu\text{-O})$, the density functional theory combined with the broken symmetry approach (DFT−BS) is adopted. The exchange coupling constants $J$ can been estimated by calculating the energy difference between the high-spin state ($E_{HS}$) and the broken-symmetry state ($E_{BS}$) (for isotropic Heisenberg spin Hamiltonian $\hat{H} = -2J\hat{S}_1\hat{S}_2$) according to the following expression.[12]

$$E_{HS} - E_{BS} = [-S_{max}(S_{max}+1) + \sum_{S}^{S_{max}} A_1(S)S(S+1)]J \quad (1)$$

where $S$ corresponds to the spin states of the molecule studied and $A_1(S)$ stands for squares of Clebsch−Gordan coefficients. In the cases of the $(Cp_2Ti)_2(\mu\text{-O})$, where $S_1 = S_2 = {}^1/_2$, we get the expression as follows:

$$E_{HS} - E_{BS} = -J \quad (2)$$

According to recent Ruiz et al. experience based on a number of calculations on the magnetic exchange coupling constants with the broken-symmetry approach,[17−19] $E_{BS}$ may be regarded as an approximation of the energy of the singlet state. Thus, the following expression for calculating the $J$ value was suggested:

$$E_{HS} - E_{BS} = -2J \quad (3)$$

where a positive value of the coupling constant $J$ indicates a triple ground state with parallel spins (i.e., ferromagnetic character) and the negative value of $J$ means antiferromagnetic behavior. In our calculations, the eq 3 is adopted.

All of the calculations have been carried out using the Amsterdam density functional (ADF) package, version 2.3.[20] The local density approximation (LDA) with local exchange and correlation potentials makes use of the Vosko, Wilk, and Nusair (VWN) correlation functional.[21] Becke's nonlocal exchange correction[22] and Perdew's nonlocal correlation correction[23] are used in each self-consistent field (SCF) consistent cycle. We adopted the IV basis sets in ADF, which contained triple-$\zeta$ basis sets for all atoms of the molecule and a polarization function from H to Ar atom. The frozen core approximation for the inner core electrons and relativistic effects are used. The orbitals up to 3p for Ti atom, up to 1s for O and C atoms are kept frozen. The numerical integration procedure applied in the calculations is the polyhedron method developed by Velde and co-workers.[24,25] The convergence standard of the system energy is smaller than $10^{-6}$ eV, reaching a precision required for the evaluation of the $J$ values.

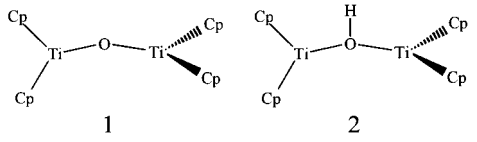


**Figure 2.** The scheme of the calculated models.

**Calculated Models.** The validity of DFT−BS for the titanium dimer studied has to be first confirmed. Hence, the experimentally determined complete structure (model **1**, see Figure 2) of $(Cp_2Ti)_2(\mu\text{-O})$ is adopted, rather than any simplified model, to allow a straightforward comparison between the calculated and experimental coupling constants. The geometry structure for the atoms of heavy elements of model **1** is directly taken from the X-ray crystallography analyses, while the partial geometry optimization for positions of all hydrogen atoms is performed. Honold et al.[7] have earlier determined the crystal structure of $(Cp_2Ti)_2(\mu\text{-O})$. As shown in Figure 1, a molecule of $(Cp_2Ti)_2(\mu\text{-O})$ consists of the two oxo-bridged $(\eta^5\text{-}C_5H_5)_2Ti$ fragments, and the $(\eta^5\text{-}C_5H_5)_2Ti$ fragments in the molecule have a typically bent sandwich geometry. As the mentioned above, the dihedral angles between the planes of the Cp rings in a $(\eta^5\text{-}C_5H_5)_2Ti$ fragment are 136.0°, where the distance of Cp−Ti is 2.067 Å. The Ti−O−Ti angle is 170.9°, and the Ti−O distance is 1.838 Å. On the basis of the model **1**, we have calculated the magnetostructural correlation by changing the Ti−O−Ti bonding angle (from 180° to 146.9°), the Ti−O distance (from 1.838 to 1.538 Å), and the dihedral angle of $Cp_2$−Ti−O−Ti−$Cp_2$ (that is dihedral angle between the two $Cp_2Ti$ fragments at 90°, 75°, 65°, 60°, 45°, 30°, 15°, and 0°).

From the model **1**, model **2** is built through protonation of the bridging oxygen ligand, leading to formation of a hydroxo OH bridging ligand, where only the O−H distance is optimized, keeping other pieces of the molecule fixed to be identical with those of model **1** to analyze the effect of different bridging ligands on the magnetic exchange interaction in the molecule. The optimized O−H distance is 0.981 Å.

## Results and Discussion

**A. Exchange Coupling Constant *J* Calculated.** The exchange coupling constant $J$ between the two titanium centers in $(Cp_2Ti)_2(\mu\text{-O})$, model **1**, is calculated to be 11.41 $cm^{-1}$ with the DFT−BS approach. The experimental value reported by Lukens and Andersen[8] is 8.3 $cm^{-1}$. The sign of the calculated $J$ value is positive. Both the experimental measurements and theoretical calculations indicate a weak ferromagnetic coupling behavior between the two titanium(III) centers in $(Cp_2Ti)_2(\mu\text{-O})$. It should be pointed out that the qualitative agreement between the experimental and calculated values for the coupling constant $J$ is good though a difference in absolute value exists. In the present paper, our purpose is placed on analysis of the dependence of magnetic exchange behavior on specific change in structures, as well as magnetic exchange mechanism. Thus, this difference in absolute value for the calculated $J$ is sufferable.

The geometrical parameters of model **1** are directly taken from structural determination experimentally as mentioned above. To further inspect the effect of the optimized geometry on the calculated $J$ value, the full geometry optimization of model **1** is performed with model **1** as an initial geometry, leading to a new model **1′**. Table 1 lists the selected optimized bond lengths and angles, as well as the calculated coupling constants $J$, by using the DFT−BS method. Table 1 reveals that, in comparison with experimental geometry, the optimized Ti−O distance is lengthened by 0.014 Å and the increment of

**TABLE 1: Selected Bond Angle, Bond Distance, and Magnetic Coupling Constant *J* for Experimental and Optimized Molecular Geometries**

| model | ∠Ti−O−Ti (deg) | $r_{Ti-O}$ (Å) | $J$ ($cm^{-1}$) |
|---|---|---|---|
| model **1** | 170.9 | 1.838 | 11.41 (calcd)<br>8.3 (exptl) |
| model **1′** | 173.3 | 1.851 | 1.29 (calcd) |

the optimized bond angle Ti−O−Ti is 2.4°. The calculated *J* value for the optimized geometry is 1.29 $cm^{-1}$, less than 11.41 $cm^{-1}$ for the geometry determined experimentally. This difference between the calculated *J* values is reasonable for the lengthened Ti···Ti distance in the optimized geometry. Both models **1** and **1′** consistently show a weak ferromagnetic exchange interaction between the two Ti(III) ions in $(Cp_2Ti)_2(\mu\text{-O})$.

**B. Protonation of the *μ*-Oxo Bridging Ligand.** The structural simplification of the molecule $(Cp_2Ti)_2(\mu\text{-O})$ with a single-atom bridge allows us to inspect definitely the effect of the bridge ligand on the magnetic exchange interaction. It has been demonstrated that in general oxo-bridged binuclear complexes of transition metals, $L_n-M-(\mu\text{-O})-M-L_n$, the antiferromagnetic coupling interaction between the two magnetic centers occurs through superexchange via the $\mu$-oxo bridging ligand, where orbital interactions between the single-occupied metal d-orbital and p-orbital on the bridging oxygen atom are responsible for the magnetic superexchange. Therefore, as soon as the protonation of the bridging oxygen atom, the p-orbital on the bridging oxygen atom and the s-orbital on the hydrogen atom form a new chemical bonding O−H and this results in weakening greatly the superexchange between metal magnetic centers.[16] However, in the case of $(Cp_2Ti)_2(\mu\text{-O})$, the ferromagnetic coupling interaction between the magnetic centers is almost not affected by the protonation of the oxo-bridge ligand. The calculated coupling constant *J* for the protonated $(Cp_2Ti)_2(\mu\text{-OH})$, model **2**, is 12.22 $cm^{-1}$, comparable with 11.41 $cm^{-1}$ for the unprotonated $(Cp_2Ti)_2(\mu\text{-O})$, model **1**. It appears that the ferromagnetic coupling interaction between the metal centers in $(Cp_2Ti)_2(\mu\text{-O})$ differs from the antiferromagnetic coupling in $L_n-M-(\mu\text{-O})-M-L_n$ in nature. The latter is involved in a weak orbital interaction through the bridging atom, but the former is an electronic potential exchange.

**C. Magnetostructural Correlation.** In the binuclear titanium metallocene $(Cp_2TiX)_2(\mu\text{-O})$,[7] in general, the Ti−O distances vary in the range 1.75−1.89 Å, and the Ti−O−Ti angles range from 162° to 180°. In the case of $(Cp_2Ti)_2(\mu\text{-O})$, the Ti−O distance is 1.838 Å and the Ti−O−Ti angle is 170.9°, close to a linear oxo-bridge. To inspect the dependence of the magnetic behavior on the Ti−O distance, *r*, and the Ti−O−Ti angle, α, the exchange coupling constants *J* with variation of the α angle and the *r* distance are calculated by using DFT−BS method.

Figure 3 is a plot of the calculated *J* values versus the Ti−O−Ti angle α in $(Cp_2Ti)_2(\mu\text{-O})$, where the α angles range from 146.9° to 180.0°. From Figure 3, it is shown that in the α variant range the exchange coupling constant *J* values are still positive, indicating no magnetic transition occurring in the ground state. And, the *J* value is insensitive to variation of the Ti−O−Ti angle. The *J* value decreases only by 2.66 $cm^{-1}$ when the α angle varies from 146.9° to 180.0°. The linear regression of the *J* values ($cm^{-1}$) with increase of the α angle can be expressed as follows:

$$J = 25.53 - 0.083\alpha \qquad (4)$$

The dependence of the calculated *J* values on the Ti−O distance *r* is shown in Figure 4, in which the exchange coupling constants retain a positive sign, indicating also a ferromagnetic character of the exchange coupling interaction in variation of the Ti−O distance. And the calculated *J* values ($cm^{-1}$) vary with an exponential function of *r* (Å):

$$J = 11.46 - 3.972 \times 10^8 \exp(-11.49r) \qquad (5)$$

The correlation coefficient is 0.9844 ranging from 1.537 to 1.837 Å.

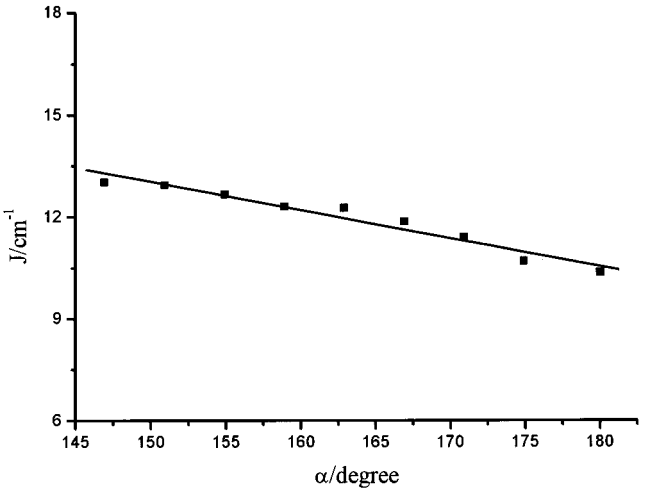


**Figure 3.** A plot of the calculated *J* value versus the Ti−O−Ti angle α.

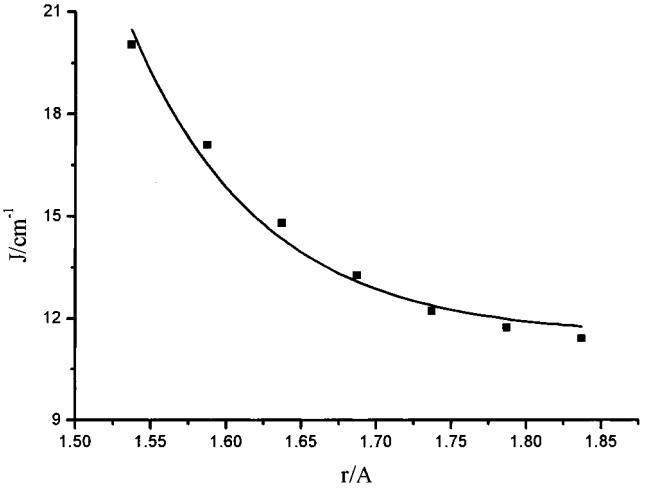


**Figure 4.** A plot of the calculated *J* value versus the Ti−O distance *r*.

The dependences of the exchange coupling constants on the Ti−O distance and the Ti−O−Ti angle in $(Cp_2Ti)_2(\mu\text{-O})$ are similar to that for $Cl_3-Fe-(\mu\text{-O})-Fe-Cl_3$ in our previous report,[16] in which the calculated *J* values are insensitive to variation of the Fe−O−Fe angle and are proportional to an exponential function of the Fe−O distance. It should be pointed out that in both $(Cp_2Ti)_2(\mu\text{-O})$ and $Cl_3-Fe-(\mu\text{-O})-Fe-Cl_3$, no transition of magnetic coupling character occurs in the variation of M−O distance and M−O−M angle. However, both the cases differ from hydroxo-bridged copper(II) dimers,[26] in which there exists a transition between ferromagnetic and antiferromagnetic coupling at the Cu−O−Cu angle of 97.5°.

**D. Dihedral Angle and Magnetic Transition.** For $(Cp_2Ti)_2(\mu\text{-O})$, a remarkable structural feature is the dihedral angle $\beta$ of 90° between the two molecular fragments $Cp_2Ti(III)$. To examine dependence of the magnetic exchange coupling on the dihedral angle $\beta$, we rotated one of the $Cp_2Ti(III)$ molecular

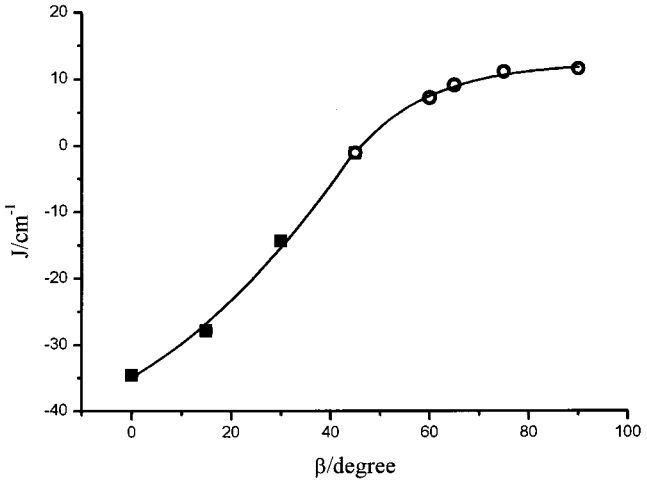


**Figure 5.** Dependence of magnetic coupling constant $J$ on the dihedral angle $\beta$.

fragments around the Ti−O bond, relative to another molecular fragment at $\beta = 0°$, 15°, 30°, 45°, 60°, 65°, 75°, and 90°. The calculated magnetic coupling constants $J$ have a continuous variation as shown in Figure 5. It is worth noting that there exists a turning point near 45°. When $\beta > 45°$, the $J$ values are positive, indicating the ground state is a triplet state, while for $\beta < 45°$, the $J$ values become negative, suggesting a singlet ground state. It is obvious that the transition of the magnetic coupling properties occurs near the dihedral angle $\beta$ of 45°, from ferromagnetic ($\beta > 45°$) to antiferromagnetic coupling ($\beta < 45°$). This magnetic transition, indeed, has been rarely observed in the magnetostructural correlation for magnetic molecules studied in previous reports. It is reminiscent of the hydroxo-bridged copper(II) dimers,[26] as mentioned above, in which the magnetic transition occurs in variation of the Cu−O−Cu bond angle α. For $\alpha > 97.5°$, the ground state is a singlet state, and for $\alpha < 97.5°$, the ground state is a triplet state. When the curve in Figure 5 is partially simulated, the following functions are obtained: when $\beta > 45°$,

$$J = -34.92 + 0.4304\beta + 0.0073\beta^2 \quad (6)$$

and when $\beta < 45°$,

$$J = 12.36 - 271.23 \exp(-0.067\beta) \quad (7)$$

For eqs 6 and 7, the correlation coefficients are 0.9961 and 0.9964, respectively. The two equations express the variation of the calculated magnetic coupling constants $J$ with the dihedral angle $\beta$ in ferromagnetic and antiferromagnetic coupling ranges, respectively. On the other hand, the small absolute values for all of the calculated coupling constants show that for either ferromagnetic or antiferromagnetic coupling the interactions between the titanium(III) centers are quite weak. Though no experimental observations for dependence of the magnetic coupling interaction on the dihedral angle $\beta$ are available, the calculations mentioned above are indeed interesting in magnetic coupling properties.

**E. Molecular Orbital Analysis.** With regard to the magnetic exchange pathway, Stucky and co-workers[4−6] have studied a number of titanocene dimers bridged by the diversified dianions of saturated and unsaturated dicarboxylic acids and have found that the antiferromagnetic couplings in these cases are mainly through superexchange via the bridging ligand. However, in the case of the oxo-bridged titanium(III) dimer, $(Cp_2Ti)_2(\mu$-O), the

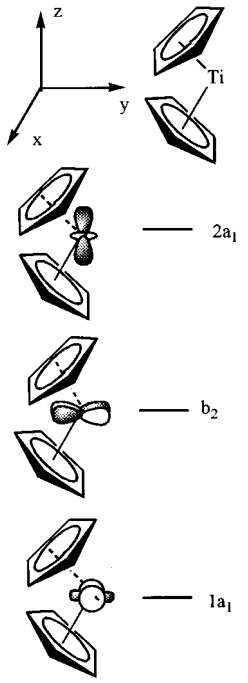


**Figure 6.** Molecular fragment orbital levels in the bent sandwich fragment $Cp_2Ti$(III).

situation differs quite from the titanocene dimers bridged by dianions of dicarboxylic acids. For $(Cp_2Ti)_2(\mu$-O), almost no effect of the bridging atom exists in magnetic exchange coupling as shown in the calculated coupling constant $J$ for the protonated $(Cp_2Ti)_2(\mu$-OH).

For a bent sandwich fragment $Cp_2Ti$(III), the low-lying levels consist mainly of the $d_{x^2-y^2}$, $d_{xy}$, and $d_{z^2}$ in order of increasing energy, in which the $d_{x^2-y^2}$ orbital with the lowest level mixes partially with the $d_{z^2}$ character because of bending back of the two parallel Cp rings. The mixture leads the electronic densities in the fragment orbital $1a_1$ to be mainly concentrated on the direction perpendicular to Ti···Ti. Figure 6 shows these fragment orbitals $1a_1$, $b_2$, and $2a_1$.[27]

On the basis of the calculations of ADF, we obtained the single-occupied molecular orbitals (SOMOs) in the triplet state with the dihedral angles $\beta = 90°$ and 0° for $(Cp_2Ti)_2(\mu$-O), shown in Figure 7, in which Figure 7a is the single-occupied molecular orbital, SOMO58 (HOMO), for $\beta = 90°$ in which an unpaired d-electron predominantly is located on a titanium center, without the participation of the bridging oxygen ligand while Figure 7b is another single-occupied molecular orbital, SOMO57 (that is the next HOMO), for $\beta = 90°$. It is evident that SOMO57 shows another unpaired d-electron to be predominantly located on another titanium center. In other words, both of the SOMOs are nonbonding orbitals in the interaction of the $1a_1$ orbitals of the $Cp_2M$ fragments with the hybrid s−p orbitals of the bridging oxygen ligand. Thus, no antiferromagnetic pathway between the two titanium centers can occur through superexchange via the bridging oxygen ligand, in contrast to Stucky's titanium dimers[4−6] mentioned above. Therefore, the only coupling pathway is the potential exchange, leading a ferromagnetic coupling.

In the case of $\beta = 0°$, the two nonbonding SOMOs mentioned above are linearly combined again to be two new SOMOs, shown in Figure 7c,d, due to the same symmetry. Consequently, the interaction between the unpaired d-electrons on the two titanium centers can occur through space, that is, the magnetic

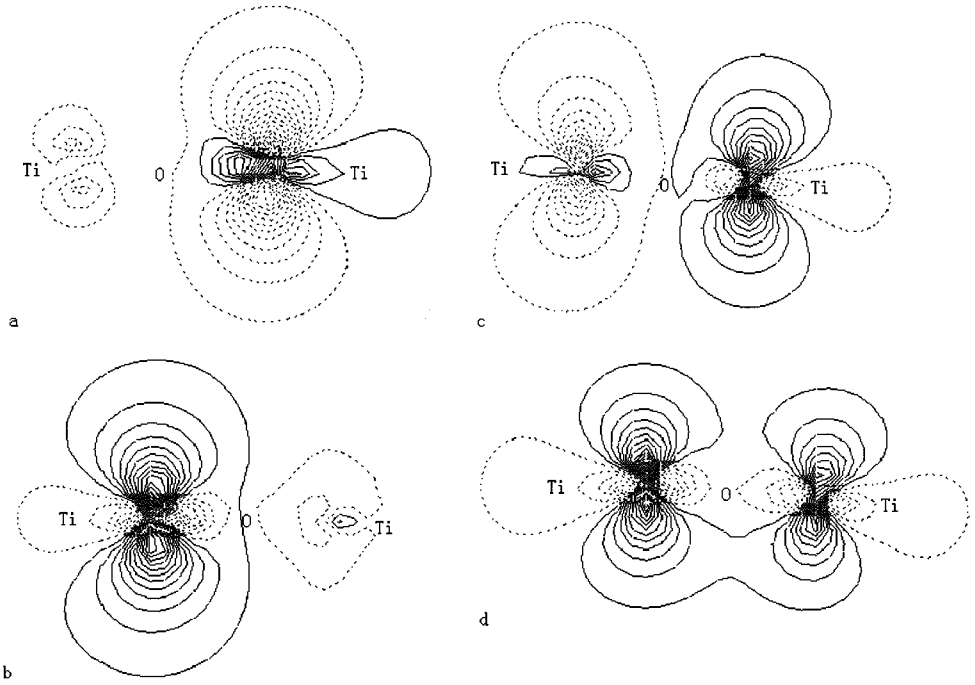


**Figure 7.** SOMOs in the triple state for $(Cp_2Ti)_2(\mu\text{-}O)$: (a) SOMO(58), $\beta = 90°$; (b) SOMO(57), $\beta = 90°$; (c) SOMO(58), $\beta = 0°$; (d) SOMO(57), $\beta = 0°$.

exchange pathway exists for the antiferromagnetic coupling between the two titanium centers for **(**$Cp_2Ti)_2(\mu\text{-}O)$.

On the basis of Hartree−Fock theory, Hay, Thibeault, and Hoffmann[28] proposed the following expression for the exchange coupling constant $J$ for a system with two metal atoms, each bearing one unpaired electron:

$$2J = 2K_{ab} - \frac{(\epsilon_1 - \epsilon_2)^2}{J_{aa} - J_{ab}} \tag{8}$$

In the eq 8, $\epsilon_1$ and $\epsilon_2$ are the energies of the singly occupied molecular orbitals (SOMOs) in the triple state and $K_{ab}$, $J_{aa}$, and $J_{ab}$ are two-electron integrals. Theoretically, the calculated coupling constant $J$ is the sum of ferromagnetic, $J_F$, and antiferromagnetic, $J_{AF}$, contributions,

$$J = J_F + J_{AF} \tag{9}$$

Thus, the first and second terms in eq 8 give the ferromagnetic and antiferromagnetic contributions to the overall coupling constant, respectively. Assuming that the two-electron terms in eq 8 are approximately constant for compounds with the same metal atoms and bridging ligand, eq 8 leads to a direct relationship between the coupling constant $J$ and the energy gap between the two SOMOs. To examine further the molecular orbital effect on the magnetic exchange interaction between the two titanium centers for $(Cp_2Ti)_2(\mu\text{-}O)$, the validity of eq 8 for the $(Cp_2Ti)_2(\mu\text{-}O)$ studied is checked by plotting the calculated $J$ values as a function of $-(\epsilon_1 - \epsilon_2)^2$. The linear dependence expected from eq 8 is found (see Figure 8), in which the regression coefficient is 0.9975. Our calculations suggest that, in the present case, the direct $1a_1|1a_1$ interaction might give rise to a variable antiferromagnetic coupling, $J_{AF}$, in the variation of the dihedral angle $\beta$ from 90° to 0°. As soon as $J_{AF} = J_F$, $J = 0$. This case is the turning point in Figure 5. When $J_{AF} < J_F$, the case becomes ferromagnetic coupling, as shown in $\beta >$ 45° of Figure 5. Also when $J_{AF} > J_F$, the system becomes antiferromagnetic coupling, as shown in $\beta <$ 45° of Figure 5.

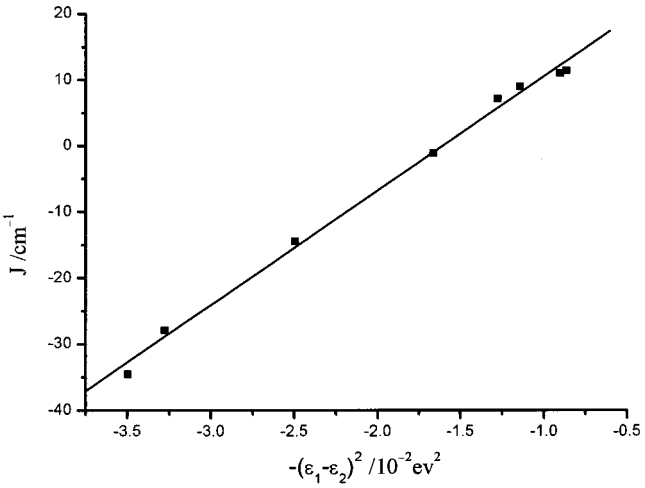


**Figure 8.** A plot of the calculated $J$ values versus $-(\epsilon_1 - \epsilon_2)^2$.

**F. Spin Population Distribution.** Except the exchange coupling constant $J$, the spin population distribution in the compound may also give some valuable hints for the magnetic exchange interaction. Table 2 gives the calculated spin population distribution on the titanium centers and the peripheral atoms in the triple state and the broken-symmetry state, for which the plus and minus signs indicate α and $\beta$ spin states, respectively. It should be mentioned that the broken-symmetry state is a mixed spin state with $Ms = 0$, not to be a pure spin state, but it represents an averaged antiferromagnetic alignment of spins. From Table 2, it is found that the spin population on each titanium atom is close to unity. It is indicated that the two titanium atoms are the magnetic centers in the molecule, which is consistent with the electronic distribution of SOMOs in Figure 7a,b. In the triplet state, the spin population on the bridging oxygen atom O1 is only −0.0717, where the opposite spin sign to the titanium atom indicates a weak spin polarization from the titanium atoms. Besides the little spin population on the bridging oxygen atom O1, the spin populations on the Cp rings also are very little, and the overall spin polarization mechanism

**TABLE 2: Spin Mulliken Populations on the Selected Atoms**

| | | HS* | | | | | BS* | | | | |
|---|---|---|---|---|---|---|---|---|---|---|---|
| atom | | s | p | d | total | spin population | s | p | d | total | spin population |
| O1 | α | 0.9716 | 2.4547 | 0.0057 | 3.4320 | −0.0717 | 0.9730 | 2.4904 | 0.0049 | 3.4683 | 0.0004 |
| | β | 0.9745 | 2.5250 | 0.0042 | 3.5037 | | 0.9731 | 2.4899 | 0.0049 | 3.4679 | |
| Ti2 | α | 0.1332 | 0.1969 | 1.7670 | 2.0971 | 1.0680 | 0.0562 | 0.1326 | 0.8465 | 1.0353 | −1.0557 |
| | β | 0.0588 | 0.1294 | 0.8409 | 1.0291 | | 0.1361 | 0.1937 | 1.7612 | 2.0910 | |
| Ti13 | α | 0.1394 | 0.2029 | 1.7728 | 2.1151 | 1.0796 | 0.1421 | 0.1996 | 1.7663 | 2.1080 | 1.0655 |
| | β | 0.0634 | 0.1348 | 0.8373 | 1.0355 | | 0.0609 | 0.1381 | 0.8435 | 1.0425 | |
| C3 | α | 0.5694 | 1.4021 | 0.0373 | 2.0088 | −0.0043 | 0.5694 | 1.4081 | 0.0356 | 2.0131 | 0.0044 |
| | β | 0.5694 | 1.4081 | 0.0356 | 2.0131 | | 0.5694 | 1.4020 | 0.0373 | 2.0087 | |
| C4 | α | 0.5725 | 1.2635 | 0.0345 | 1.8705 | −0.0122 | 0.5736 | 1.2740 | 0.0339 | 1.8815 | 0.0098 |
| | β | 0.5735 | 1.2753 | 0.0339 | 1.8827 | | 0.5725 | 1.2647 | 0.0345 | 1.8717 | |
| C5 | α | 0.5717 | 1.2763 | 0.0363 | 1.8843 | −0.0141 | 0.5735 | 1.2889 | 0.0352 | 1.8976 | 0.0125 |
| | β | 0.5734 | 1.2898 | 0.0352 | 1.8984 | | 0.5717 | 1.2771 | 0.0363 | 1.8851 | |
| C6 | α | 0.5617 | 1.2950 | 0.0381 | 1.8948 | −0.0023 | 0.5623 | 1.2981 | 0.0365 | 1.8969 | 0.0021 |
| | β | 0.5622 | 1.2983 | 0.0366 | 1.8971 | | 0.5616 | 1.2951 | 0.0381 | 1.8948 | |
| C7 | α | 0.5429 | 1.2850 | 0.0384 | 1.8663 | 0.0127 | 0.5414 | 1.2716 | 0.0384 | 1.8514 | −0.0171 |
| | β | 0.5416 | 1.2736 | 0.0384 | 1.8536 | | 0.5430 | 1.2872 | 0.0383 | 1.8685 | |
| C8 | α | 0.5396 | 1.2598 | 0.0411 | 1.8405 | −0.0147 | 0.5411 | 1.2733 | 0.0405 | 1.8549 | 0.0144 |
| | β | 0.5410 | 1.2737 | 0.0405 | 1.8552 | | 0.5395 | 1.2599 | 0.0411 | 1.8405 | |
| C9 | α | 0.5507 | 1.3745 | 0.0401 | 1.9653 | −0.0259 | 0.5538 | 1.3972 | 0.0392 | 1.9902 | 0.0240 |
| | β | 0.5537 | 1.3983 | 0.0392 | 1.9912 | | 0.5505 | 1.3756 | 0.0401 | 1.9662 | |
| C10 | α | 0.5636 | 1.3035 | 0.0372 | 1.9043 | 0.0103 | 0.5629 | 1.2948 | 0.0359 | 1.8936 | −0.0110 |
| | β | 0.5629 | 1.2952 | 0.0359 | 1.8940 | | 0.5636 | 1.3039 | 0.0371 | 1.9046 | |
| C11 | α | 0.5621 | 1.2976 | 0.0372 | 1.8969 | 0.0038 | 0.5617 | 1.2936 | 0.0373 | 1.8926 | −0.0049 |
| | β | 0.5617 | 1.2941 | 0.0373 | 1.8931 | | 0.5622 | 1.2981 | 0.0372 | 1.8975 | |
| C12 | α | 0.5623 | 1.2945 | 0.0395 | 1.8963 | 0.0001 | 0.5625 | 1.2955 | 0.0382 | 1.8962 | −0.0005 |
| | β | 0.5626 | 1.2954 | 0.0382 | 1.8962 | | 0.5623 | 1.2949 | 0.0395 | 1.8967 | |

[a] HS = high-spin state; BS = broken-symmetry state.

in the molecule determinates plus or minus sign for the spin on the carbon atoms. But the spin alternate sign is not regular because of the bent sandwich geometry of the $Cp_2Ti$ fragment. It is evident that the spin populations on the titanium atoms predominantly come from d-orbital, though there exists a little contribution from s- and p-orbitals. This is also consistent with the d-orbital characteristic of the SOMOs in Figure 7a,b.

## Conclusions

The weak ferromagnetic coupling and the dihedral angle $\beta$ of 90° between the two $Cp_2Ti$ fragments are the two salient features for the simplest binuclear titanium(III) metallocene, $(Cp_2Ti)_2(\mu\text{-O})$. The calculations based on the ADF−BS approach and molecular orbital analyses show that neither antiferromagnetic pathway through superexchange via the bridging atom nor direct through-space interaction between Ti···Ti exist in $(Cp_2Ti)_2(\mu\text{-O})$. This explains the weak ferromagnetic coupling for $(Cp_2Ti)_2(\mu\text{-O})$. In the further inspection of variation of the dihedral angle $\beta$, it is found that as the dihedral angle $\beta$ ranges from 90° to 0° the direct through-space interaction between Ti···Ti occurs, leading the $J_{AF}$ component to increase gradually. When $\beta > 45°$, $J_{AF} < J_F$, namely, ferromagnetic coupling. On the other hand, if $\beta < 45°$, $J_{AF} > J_F$, namely, antiferromagnetic coupling.

**Acknowledgment.** This project is supported by the National Nature Science Foundation of China (Grants 29831010 and 20023005) and State Key Project of Fundamental Research of China (Grant G1998061305). The authors thank Dr. Noodleman (The Script Research Institute, U.S.A.) and Dr. Jian Li for introduction on the broken-symmetry approach.

## References and Notes

(1) Kolczewski, CH.; Fink, K.; Staemmler, V. *Int. J. Quantum Chem.* **2000**, *76*, 137.
(2) Weihe, H.; Gudel, H. U. *J. Am. Chem. Soc.* **1998**, *120*, 2870.
(3) Fink, K.; Fink, R.; Staemmler, V. *Inorg. Chem.* **1994**, *33*, 6219.
(4) Francesconi, L. C.; Corbin, D. R.; Clauss, A. W.; Hendrickson, D. N.; Stucky, G. D. *Inorg. Chem.* **1981**, *20*, 2059.
(5) Kramer, L. S.; Clauss, A. W.; Francesconi, L. C.; Corbin, D. R.; Hendrickson, D. N.; Stucky, G. D. *Inorg. Chem.* **1981**, *20*, 2070.
(6) Francesconi, L. C.; Corbin, D. R.; Clauss, A. W.; Hendrickson, D. N.; Stucky, G. D. *Inorg. Chem.* **1981**, *20*, 2078.
(7) Honold, B.; Thewalt, U.; Herberhold, M.; Alt, H. *J. Organomet. Chem.* **1986**, *314*, 105.
(8) Lukens, W. W., Jr.; Andersen, R. A. *Inorg. Chem.* **1995**, *34*, 3440.
(9) Ruiz, E.; Alemany, P.; Alvarez, S.; Cano, J. *J. Am. Chem. Soc.* **1997**, *119*, 1297.
(10) Ruiz, E.; Cano, J.; Alvarez, S.; Alemany, P. *J. Am. Chem. Soc.* **1998**, *120*, 11122.
(11) Adamo, C.; Barone, V.; Bencini, A.; Totti, F.; Ciofini, I. *Inorg. Chem.* **1999**, *38*, 1996.
(12) Noodleman, L. *J. Chem. Phys.* **1981**, *74*, 5737.
(13) Noodleman, L.; Baerends, E. J. *J. Am. Chem. Soc.* **1984**, *106*, 2316.
(14) Noodleman, L.; Case, D. A. *Adv. Inorg. Chem.* **1992**, *38*, 423.
(15) Li, J.; Noodleman, L.; Case, D. A. In *Inorganic Electronic Structure and Spectroscopy*; Solomon, E. I., Lever, A. B. P., Eds.; Wiley: New York, 1999; Vol. I, p 661.
(16) Chen, Z.; Xu, Z.; Zhang, L.; Yan, F.; Lin, Z. *J. Phys. Chem. A* **2001**, *105*, 9710.
(17) Ruiz, E.; Alemany, P.; Alvarez, S.; Cano, J. *Inorg. Chem.* **1997**, *36*, 3683.
(18) Ruiz, E.; Cano, J.; Alvarez, S.; Alemany, P. *J. Comput. Chem.* **1999**, *20*, 1391.
(19) Rodriguez-Fortea, A.; Alemany, P.; Alvarez, S.; Ruiz, E. *Chem.—Eur. J.* **2001**, *7*, 627.
(20) *Amsterdam Density Functional (ADF)*, version 2.3; Scientific Computing and Modelling, Theoretical Chemistry, Virje Universiteit: Amsterdam, The Netherlands, 1997.
(21) Vosko, S. H.; Wilk, L.; Nusair, M. *Can. J. Phys.* **1980**, *58*, 1200.
(22) Becke, A. D. *Phys. Rev. A* **1988**, *38*, 3098.
(23) Perdew, A. D. *Phys. Rev. B* **1988**, *33*, 8822.
(24) Boerrigter, P. M.; Velde, G. T.; Baerends, E. J. *Int. J. Quantum Chem.* **1988**, *33*, 87.
(25) Velde, G. T.; Baelends, E. J. *J. Comput. Phys.* **1992**, *99*, 84.
(26) Kahn, O. *Molecular Magnetism*; VCH Publisher: New York, 1993; p 160.
(27) Albright, T. A.; Burdett, J. K.; Whangbo, M.-H. *Orbital Interaction in Chemistry*; Wiley: New York, 1985; p 395.
(28) Hay, P. J.; Thibeault, J. C.; Hoffmann, R. *J. Am. Chem. Soc.* **1975**, *97*, 4884.